

Sulfited Tannin Capsules: Novel Stimuli-Responsive Delivery Systems

Luc Zongo, Heiko Lange,^{*,#} and Claudia Crestini^{*,#}Cite This: *ACS Omega* 2021, 6, 13192–13203

Read Online

ACCESS |



Metrics & More

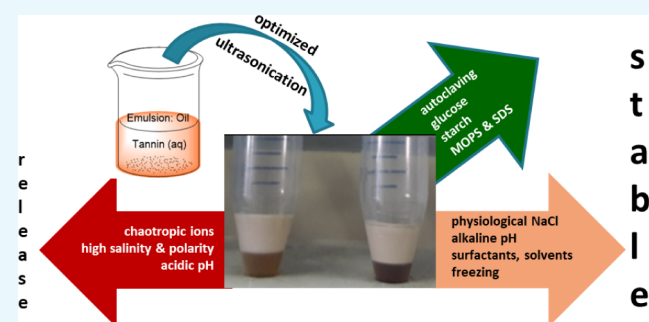


Article Recommendations



Supporting Information

ABSTRACT: Microcapsules of sulfited *Acacia mearnsii* tannin (AmST-MCs) were generated for the first time via the sonochemical method. Their stability profile was assessed and set in the general context of tannin microcapsules (TMCs) generated under the same experimental conditions. The analytical data gathered in this work indicate an excellent stability of TMCs over time as well as under high temperature and pressure, which is a major milestone toward the meaningful applications of TMCs in industrial, pharmaceutical, and biomedical applications in which sterilization of TMCs might be a prerequisite. Active release is shown to be efficiently triggered by varying pH and/or salinity, with different profiles for TMCs from sulfited and nonsulfited species. Surfactants also affect the stability of TMCs significantly, with effects eventually amplifiable by pH and the inherent kosmotropic and chaotropic characteristics of salt components in solutions.



INTRODUCTION

Microencapsulation techniques are of significant interest in academic and industrial research.^{1–5} As per definition, a microcapsule (MC) is a particle with a core–shell structure in which the core can be a solid, liquid, or gaseous system and the shell can be a polymer system or an inorganic material.^{4,6,7}

MCs are widely used in applications in which an active compound needs to be protected from environmental factors such as UV radiation, oxygen, moisture, and reactive species, both during shelf life and during application until the point of action is reached. In biomedical and pharmaceutical applications, MCs can be used when a controlled release is needed or a premature metabolization/action of the encapsulated active is to be prevented. For instance, controlled release of an active medical agent can be a means to make available the drug over a longer period of time to achieve, e.g., a once-daily dosing of a drug. Side effects of drugs can be eventually reduced by means of encapsulation, especially when used together with targeted delivery approaches.^{1,2,1,1,5}

Tannin-based encapsulation systems recently gained attention for the purpose of developing novel types of delivery systems for actives with inherent potential for synergistic effects in addition to an ideally unique stimuli responsiveness.^{8–15} Tannins represent a readily available sustainable resource from agricultural and forestry residues.^{16,17} For decades, they have been a relevant subject of research because of their essential contribution to plant physiology, providing plants with resistance to pathogens and predators, and their antioxidant abilities, free-radical-scavenging capacity, and potential effects on human health.^{16–18} Being present in

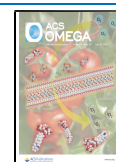
most of the higher plants around the globe and in almost all parts of the plants, i.e., in seeds, roots, bark, wood, and leaves,¹⁷ these secondary metabolites are classified according to some leading structural/chemical features. As plant polyphenols, in general, tannins in particular provide protection against a wide range of biotic and abiotic stresses, possesses antioxidant and antiinflammatory properties, exhibit antimutagenic and anticarcinogenic activities, prevent and delay cardiovascular diseases, increase the lifespan, and retard the onset of age-related markers.^{18,19} Tannins thus naturally respond to important requirements of ideal MC shell materials when aiming at applications that would benefit from synergistic effects in the fields of biomedicine, pharmaceutical applications, and cosmesis:^{17,20,21} (a) biocompatibility, (b) antioxidant activity, (c) synergistic potential for enhancing the activity of encapsulants, (d) amphiphilic characteristics, and (e) propensity to effective electronic interactions for the formation of supramolecular structures.

Given that hydrolyzable tannins (HTs) and condensed tannins (CTs) constitute more than 90% of the total world production of commercialized tannins, representing chemically and economically interesting biopolymers, an initial ultra-

Received: February 26, 2021

Accepted: April 29, 2021

Published: May 11, 2021



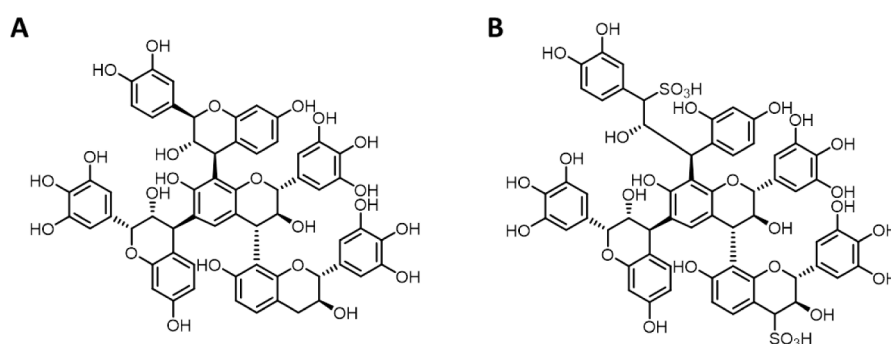


Figure 1. Exemplary structural features of tetramers of (A) the *Acacia mearnsii* bark extract (*AmT*)²⁹ and (B) *Acacia mearnsii* sulfited tannin (*AmST*).²⁸

Table 1. Representative Results of the Optimization Sequence for a Scalable *AmST*-MC and *AmT*-MC Production^a

entry	deprotonation equivalence ^b	pH aqueous T solution	ratio of system	AUL Ø (µm)		min–max Ø (µm)		PDI		# MCs (10 ¹² MCs/mL)	
				<i>AmST</i>	<i>AmT</i>	<i>AmST</i>	<i>AmT</i>	<i>AmST</i>	<i>AmT</i>	<i>AmST</i>	<i>AmT</i>
1	n.d. ^c	n.d. ^c	10:1		1.40		0.50–4.10		0.4		0.0024
2	0.0	4.5	10:1	1.43	1.34	0.27–3.99	0.25–3.74	0.6	0.6	0.12	0.13
3	0.0	4.5	1:1	1.11	0.98	0.35–4.47	0.31–3.95	0.6	0.7	0.29	0.35
4	0.1	7.4	1:1	1.39	1.37	0.28–3.69	0.28–3.64	0.5	0.6	0.87	0.81
5	0.25	9.5	1:1	1.18	0.94	0.35–3.74	0.28–2.98	0.7	0.7	1.76	1.90
6	0.50	10.5	1:1	1.50	1.44	0.27–3.73	0.26–3.58	0.5	0.4	2.03	2.14
7	0.75	11.5	1:1	1.54	1.40	0.29–4.21	0.26–3.83	0.6	0.6	3.86	3.66

^aThe systems were magnetically stirred for 5 min and then treated by ultrasonication at 160 W (40% amplitude) for 10 min. ^bDeprotonation equivalence of the phenolic groups based on the previously published structural analysis of *AmT*²⁹ using aqueous 1 M NaOH solution. Applying the same analysis protocol reported before²⁹ and detailed in the Supporting Information to *AmST*, a total phenol content of 6.40 mmol/g was obtained. ^cUsing previously reported settings.⁸

sound-based,^{22,23} template-free protocol for the generation of micro- and nanocapsules on the basis of tannins saw mainly the implementation of these two fundamental tannin classes; however, complex tannins (CXTs) have also been successfully employed later on.^{8,9}

Although the general suitability of tannins as shell materials seems to be independent of the specific structural features of HTs, CTs, and CXTs, pointing as such to the polyphenolic character as the main element for stacking propensities and hence reported MC formation, studies on lignin-based systems have revealed interesting differences in the actual MC stability as a function of the presence of different pH-sensitive groups, for example.²⁴ The development of fine-tuned tannin microcapsules (TMCs) for specific applications consequently needs to be based on a more fundamental and detailed understanding of the connection between specific structural features and observable detailed TMC stability profiling. To not additionally complicate analyses, CTs were chosen as the working horse tannin class due to their chemically more stable structure in comparison with HTs so as to consequently establish the stimuli responsiveness of tannin-based MCs as a function of specific structural features. TMCs reported so far have been realized based predominantly on electronic interactions involving aromatic moieties and phenolic OH groups in tannins. Introduction of a third, differently pH-sensitive group such as a sulfone group was envisaged to add novel and additional modes of intermolecular interactions to TMCs, thus presumably increasing the number of potential fields of applications. Such a differently pH-sensitive group, with respect to typical tannin functional groups, is the sulfone group.

To add this novel functional group to the TMC system, sulfited *Acacia mearnsii* (*AmST*) tannin was chosen as the capsule building blocks.

Despite the fact that sulfited tannins are readily available,^{17,20} they have only been scarcely used in valorization applications.^{20,25–27} To achieve a mapping of general TMC stability as a function of structural properties for creating a rational base for purposeful TMC applications, the presence of the sulfonate functional groups in sulfited tannins is extremely relevant since it interestingly increases the naturally present amphiphilic character by the explicit introduction of negative charges over an extended pH range in the tannin. It was anticipated that such a rather drastic change allows for generating TMCs that display a wider range of stability profiles. With an extended stability profile, it will be easier to choose the most appropriate TMC system for any type of application that might require a fast disintegration, i.e., an accelerated release, an elevated stability, i.e., a slow release, or a fundamental stability under one set of specific conditions to fully disintegrate with abrupt changes in these conditions, as, for example, needed when orally taken drugs pass through the stomach to reach their destination in the intestine.

Acacia mearnsii bark tannin (*AmT*) as a typical representative for a CT and *AmST* as a typical example for sulfited condensed tannins (SCTs) were consequently chosen based on the available supporting background knowledge from our previous work and based on the archival literature;^{28,29} Figure 1 shows an overview of the suggested and proven general and specific structural aspects of the two tannin species based on previous findings and new analysis (Figure S1).

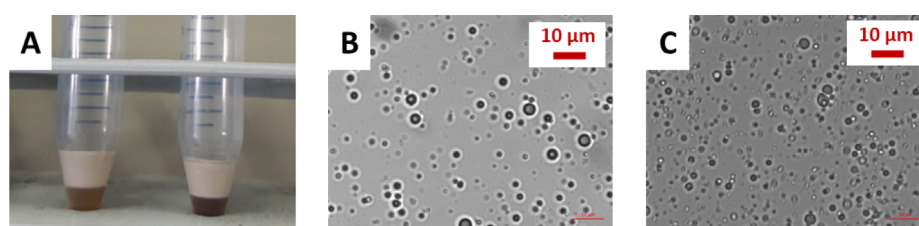


Figure 2. (A) *AmST*-MCs (left) and *AmT*-MCs (right) produced under optimized conditions prior to isolation; (B) exemplary microscopic image of *AmST*-MCs; and (C) exemplary microscopic image of *AmT*-MCs.

Table 2. Assessment of *AmST*-MC and *AmT*-MC Stability under Various Storing Conditions

entry	pressure (mbar)	temperature (°C)	time	AUL Ø (μm)		PDI		# MCs (10 ¹² MCs/mL)		stability index ^a	
				<i>AmST</i>	<i>AmT</i>	<i>AmST</i>	<i>AmT</i>	<i>AmST</i>	<i>AmT</i>	<i>AmST</i>	<i>AmT</i>
1	~1000	23	1 h	1.44	1.28	0.5	0.5	6.97	6.64	1.00	1.00
2	~1000	23	1 d	1.44	1.28	0.5	0.5	6.97	6.64	1.00	1.00
3	~1000	23	180 d	1.50	1.30	0.5	0.5	6.83	6.52	0.99	0.98
4	2026	121	30 m	1.50	1.30	0.5	0.5	6.90	6.52	0.99	0.98
5	~1000	-20	7 d	1.76	1.72	0.5	0.3	2.51	3.25	0.36	0.49

^aDetermined as the ratio between the number of capsules before and after exposure to specified conditions.

This study thus describes, for the first time, the synthesis of novel sulfited tannin MCs (STMCs) and a comprehensive survey of the stimuli-triggered cleavage in comparison with nonsulfited tannin MCs (TMCs) under selected physical and chemical conditions, including time, temperature, pressure, pH, salinity, biomacromolecules, and surfactants and solvent effects. For the liquid core of the capsules, refined olive oil was chosen once more, and the capsules were generated by applying the previously established sustainable sonication method.

RESULTS AND DISCUSSION

Generation of Microcapsules from Sulfited and Unmodified *Acacia mearnsii* tannin. While in previous studies principal generations of TMCs have been demonstrated,^{8,9} this work started with identifying the best conditions for generating sulfited tannin MCs, maintaining the principal approach via the ultrasonication method (Figure S2). The criteria for judging whether optimum conditions were reached comprised the number of capsules generated as well as their size and the polydispersity. By varying methodically the pH of the aqueous *AmST* starting solution, *AmST* concentration, the water/oil ratio of the solution to be sonicated, and ultrasonication power and time, *AmST*-MCs as well as *AmT*-MCs have been generated. The details of the optimization study are given in Table 1. The analysis of the generated capsules was performed using the straight forward optical microscope-based analysis protocol established before and outlined once again in the Experimental Section of this work.^{8,9}

In this *ex novo* optimization process, a 1:1 mixture of an aqueous *AmST* solution at a concentration of 0.5% w/v at pH ~12 was found to be the best for being mixed with the oily phase; the tannin concentration was thus confirmed with respect to earlier studies, while the pH was found to be much more crucial for efficient capsule formation. Initial emulsion formation was achieved prior to sonication by magnetically stirring the water–oil mixture for 5 min at moderate speeds between 800 and 1000 rpm. Ultrasonication of the emulsion at 160 W (40% amplitude) for 10 min was found to be the most efficient energy input for the generation of *AmST*-MCs that

could be generated in large numbers. Figure 2 shows the photographs and typical microscopic images of the generated *AmST*-MCs and *AmT*-MCs.

As outlined in Table 1, this approach, when applied to a nonsulfited *Acacia mearnsii* tannin, *AmT*, used already in previous studies, resulted in a significant increase in the number of *AmT*-MCs (Table 1, entries 1 and 2): the number of TMCs increases from 2.4×10^9 to 6.64×10^{12} MCs/mL, i.e., by 3 magnitudes using the optimized settings with respect to previous results.⁸ Moreover, the optimized setup offers a 5 times higher volume of isolated and “concentrated,” i.e., densely packed, *AmT*-MCs.

Fundamental Morphological Characteristics. Microscopic analyses of both *AmST*-MCs and *AmT*-MCs confirm a morphological appearance that was expected based on various previous works. The sulfonate groups present in *AmST* appear to have no obvious effect on morphological features; only the radius of *AmST*-MCs generally seems to be enlarged by approx. 10–15% compared to that of *AmT*-MCs. Previous studies revealed that the shell is very thin, accounting for approx. 1–2% of the capsule diameter in the case of a nonsulfited condensed tannin that is structurally similar to *AmT*;⁸ it can be expected that the *AmT*-MCs show similar characteristics under comparable analysis conditions. Given the overall similarity in the fundamental structural characteristics between the tannins, and thus a similarity in terms of fundamental aggregation properties, given further the fact that equal amounts of tannins have been used for capsule generation in also otherwise unchanged conditions, and given further that the capsule yields are comparable in terms of magnitudes, it can be assumed that the novel *AmST*-MCs also have only a very thin shell and that the presence of the sulfonate groups does not drastically change this feature that characterizes more generally the capsules formed via the ultrasonication approach using polyphenols for shell formation.^{8,30}

TMCs under Storing Conditions. The principal stability of MCs under storage conditions, as such closely related to shelf life features, normally guides the choice for the specific shell component alongside with the intended purpose of

Table 3. Assessment of the Effect of Typical Excipients on the Stability of AmST-MCs and AmT-MCs

entry	excipient	pH	time (h)	salinity (ppt)	AUL $\bar{\phi}$ (μm)		PDI		# MCs (10^{12} MCs/mL)		stability index ^a	
					AmST	AmT	AmST	AmT	AmST	AmT	AmST	AmT
1	H ₂ O [reference]	~7			1.44	1.28	0.5	0.5	6.97	6.64	1.00	1.00
2	AE-25 ^b	7	8		1.38	1.47	0.4	0.5	3.76	3.86	0.54	0.85
3	AE-25	7	24		1.50	1.43	0.5	0.4	3.30	3.40	0.47	0.75
4	AE-25	7	48		1.52	1.32	0.4	0.3	3.10	2.37	0.45	0.52
5	AO ^c	8	8	54	1.39	1.66	0.4	0.5	7.02	3.86	1.0	0.85
6	AO	8	24	54	1.27	1.73	0.3	0.6	6.98	4.07	1.0	0.90
7	AO	8	48	54	1.14	1.59	0.4	0.5	6.99	3.68	1.0	0.81
8	MOPS ^d	~7	48	21	1.35	1.61	0.4	0.6	6.93	4.09	0.99	0.90
9	SDS ^e	~7	48	29	1.38	1.58	0.3	0.4	5.28	2.50	0.76	0.73
10	glucose ^f	~7	48		1.42	1.31	0.5	0.4	6.55	6.17	0.94	0.93
11	starch	~7	48		1.30	1.40	0.5	0.5	6.60	6.30	0.95	0.90
12	EtOH ^g		48									
13	NaCl (aq) ^h	7	48	9	1.37	1.46	0.4	0.5	3.83	4.98	0.55	0.75

^aDetermined as the ratio between the number of capsules before and after exposure to specified conditions. ^bFatty alcohol ethoxylate. ^cAlkyl amine oxide. ^d3-(*N*-Morpholino)propanesulfonic acid. ^eSodium dodecyl sulfate. ^fPhysiological solution of glucose (5% w/v). ^gEthanol. ^hPhysiological solution of NaCl (9% w/v).

microencapsulation.^{1,31} As reported in Table 2, entries 2–5, freshly synthesized and 6 months old AmST-MCs and AmT-MCs generated via the optimized scalable method display practically identical and visual statistical quantitative characteristics, in the range of the average error determined for the selected statistical quantitative analysis. A long shelf life in the deionized neutral aqueous systems seems thus guaranteed. Any other conditions, however, might well affect the STMC and TMC stability.

Pharmaceutical products are eventually subjected to processing and/or storing preparation steps involving (deep-) freezing, drying, pasteurization, or sterilization. Subjecting STMCs and TMCs to exemplary sterilization and freezing procedures, it was found that AmST-MCs and AmT-MCs in terms of morphology and statistical key numbers were not affected by autoclaving. On the contrary, in line with the behavior of lignin MCs,²⁴ ~40% and 50% of AmST-MCs and AmT-MCs, respectively, did not withstand freezing (Table 2, entry 4).

Stability of TMCs in the Presence of Common Excipients and Surfactants. Tannins provide an invaluable opportunity for the development of MC systems in the biomedical field. TMCs containing pharmacologically active substances can easily be imagined to be part of a drug formulation. Such preparations commonly contain one or more pharmacologically inactive excipients, comprising mono, di, and polysaccharides, surfactants, or simple solvents in the case of liquid preparations. Both AmST-MCs and AmT-MCs stabilities were thus tested against some of these excipients to investigate the effect of such matrix elements on TMC integrities. Table 3 gives an overview of the results obtained in these tests. The microscopic images shown in Figures S3 and S4 illustrate the changes observed in the capsule quantity and morphology in the case of AmST-MCs and AmT-MCs, respectively, when brought into contact with the agents listed in Table 3.

In the aqueous solution of fatty alcohol ethoxylate (AE-25) at neutral pH, ~50% of AmST-MCs were disassembled after the first 8 h of incubation time; in the case of AmT-MCs, a similar trend, albeit to a slightly lesser extent, was observed (Table 3, entries 2–4). These results indicate that nonionic

surfactants may significantly affect the stability of Am(S)T-MC via a common swelling mechanism indicated by the increasing size of remaining capsules. Mechanistically, this swelling could be the result of the two-step process: initially, the surfactant was imagined to intercalate between the shell form in tannin molecules, causing the shell to become more porous. Once pore sizes permit a transition of surfactant molecules, the surfactant might additionally penetrate the shell to dilute the oily core following simple chemical gradients emerging from the polar aqueous environment and the hydrophilic interior.

When aqueous amphoteric surfactants were tested in the form of a standard alkyl amine oxide (AO) at pH 8 and a salinity of 54 ppt, AmST-MCs performed significantly better than AmT-MCs; while the latter was disassembled to ca. 15%, sulfited species showed an excellent stability index even after prolonged exposure times (Table 3, entries 5–7). Aqueous MOPS solutions showed similar trends. In the case of the amphoteric surfactants, however, the morphological changes that the two different capsule systems undergo are opposite in terms of the capsule size: AmST-MCs show a clear shrinkage, while AmT-MCs increase in diameter. This observation can be directly linked to the presence of the sulfonate groups in AmST-MC shells. No oil residues are observed in the samples, indicating that the numerical stability reflects true capsule stability as such and hence also indicating that observable shrinkage is not caused by the loss of oil from the core but caused by a shell that became more porous due to the presence of amphoteric surfactant. Shrinkage rather presents a tightening of the capsule shell in the complex environment. In the case of AmT-MCs, however, the surfactant seems to weaken the shell once more, leading to a dilution of the core and final bursting.

Aqueous solutions containing sodium dodecyl sulfate (SDS) trigger a slow disassembly and thus slow active release in both sulfited and nonsulfited MCs (Table 3, entry 9) in both systems. Once again opposite changes of capsule sizes are observed, with AmST-MCs slightly shrinking and AmT-MCs seem to grow. While the alkylsulfonate residue can be assumed to act in a similar fashion to the amphoteric surfactants, the presence of the sodium cation additionally complicates the

situation eventually; this aspect is discussed in more detail in the section dedicated to salinity effects (*vide infra*).

In a 5% w/v aqueous glucose solution, corresponding to the standard glucose concentration in intravenous administrations, both *AmST*-MCs and *AmT*-MCs were substantially stable (Table 3, entry 10). In addition, TMC preparations were perfectly stable in aqueous starch solution. Over a period of 48 h, no reduction in the capsule numbers was detected, independently of whether a sulfited or nonsulfited condensed tannin was used (Table 3, entry 11).

The results obtained by testing the ionic surfactants indicated already that salinity has a notable effect on capsule stability and integrity and thus inevitably on the release properties. This was further investigated using specific salt solutions. In a physiological solution of sodium chloride, TMCs of both sulfited and nonsulfited tannins show only moderate stabilities. Destructive effects are higher in the case of *AmST*-MCs, where only 50% survived the first 48 h in the saline environment. *AmT*-MCs would be released with slower kinetics: only 25% of the capsules are lost.

The stabilities of *AmST*-MCs and *AmT*-MCs have been assessed further in light of potential industrial applications: TMC stability was investigated in the presence of mixtures of functional organic macromolecules such as enzymes, phospholipids, etc. Detailed results are presented in Tables S1 and S2. These studies revealed that they are very stable in the aqueous solutions containing purified proteins, *i.e.*, BSA. In more complex environments containing mixtures of proteins and salts, stability drops gently. Noteworthy, *AmST*-MCs do show a higher stability than the corresponding *AmT*-MCs. The amount of capsule loss in the case of *AmT*-MCs was found to parallelize an increase in the mean capsule diameter (Table S3). This suggests that a gradual swelling till burst-type of mechanism, rather than a more or less spontaneous disintegration occurs. Shell-forming intermolecular interactions between SCTs must, in turn, be less susceptible to interference by physiological substances, hinting once again at a beneficial effect of the presence of the sulfonate groups. This could be due to an active participation of these groups in the intermolecular interactions or due to a changed surface characteristic of the capsules that hampers, on the basis of electrostatic repulsions, the approach of physiological macromolecules that, assuming an intercalation as principle action underlying capsule inflation, would ultimately destroy the TMCs.

The experimental results collected to this point unequivocally indicate a TMC disassembly for controlled active release that can be triggered by (a) pH, which has been used in the past as an obvious means to trigger TMC disassembly and release of actives;^{8,9} (b) connected factors such as the nature of cations and anions and salinity, in general; and (c) the nature of the solvents, *i.e.*, protic or aprotic, polar or apolar. In particular, the pH and salinity dependence of the TMC stability was thus tested in greater detail, as discussed in the following sections.

pH-Triggered Disassembly of *AmST*-MCs and *AmT*-MCs.

Similar to most of the macromolecules, the TMC shell is electrically charged even if the overall system is electrically neutral; this is especially true in case of the sulfited tannin. Therefore, if the TMC shell is slightly charged, the electrostatic repulsion and the intermolecular repulsion will be minimized, favoring, as consequence, the TMC shell stability.

Changes in pH can be used in appropriate systems to accentuate or inhibit the stability of colloidal suspensions, interfering with the electrostatic forces that govern the stability of particle systems and colloidal solutions.³¹ The pK_a of the catechin-based CTs is ~ 9 , reflecting their polyphenolic character.²¹ Consequently, from pH 1 to 9, *AmT* moieties are mainly protonated, being thus neutral throughout the TMC shell. In the case of the sulfited tannin, with the sulfonate groups ($pK_a \sim 2$) being deprotonated under any conditions apart from pH 1–2, the TMC shell displays much higher loads of internal electrostatic repulsions over practically the entire pH range. Ion–dipole interactions in the form of “anion– π ” and “cation– π ” interactions are also expected to be present in the TMC shells.³² The intramolecular electrostatic interactions between the cations present in the TMC shell, *i.e.*, H^+ (autodissociation and buffer), K^+ or Na^+ (buffers), and the tannin-inherent dipoles (π systems), all being sensitive to changes in the pH and nature of buffer systems used, are consequently expected to vary and create different stability profiles of the two different capsule systems under study, *i.e.*, *AmST*-MCs and *AmT*-MCs.

Stability tests across the entire pH range, realized using various buffer solutions (Table S3), show noteworthy TMC stability, vastly independent of the tannin nature only in the neutral to alkaline pH range (Figure 3 and Table 4). Figures S5 and S6 show the response of *AmST*-MCs and *AmT*-MCs, respectively, to various pH values listed in Table 4.

The *de facto* complete disassembly of the *AmST*-MCs can be explained by a destabilizing effect of “cation– π ” interactions

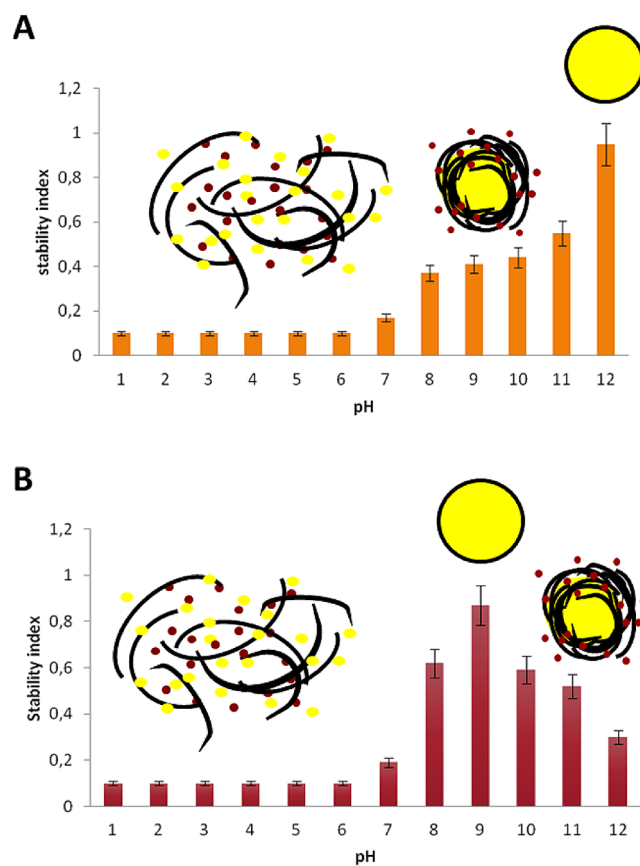


Figure 3. (A) pH-dependent cleavage of *AmST*-MCs and (B) pH-dependent cleavage of *AmT*-MCs.

Table 4. Assessment of the pH-Dependent Stability of AmST-MCs and AmT-MCs^a

entry	buffer system ^b	pH	salinity (ppt)	chaotropic (mM)	chaotropic (%)	kosmotropic (mM)	kosmotropic (%)	AUL ϕ (μm)		PDI		# MCs (10^{12} MCs/mL)		stability index				
								AmST	AmT	AmST	AmT	AmST	AmT	AmST	AmT			
1	KCl/HCl	1	4.8	K ⁺ [29.0] H ⁺ [100.0]	100											<0.10	<0.10	
2	KCl/HCl	2	5.8	Cl ⁻ [100.0] K ⁺ [56.8] H ⁺ [10.0]	100												<0.10	<0.10
3	CH ₃ COOH/CH ₃ COONa	3	6.0	Cl ⁻ [100.0] Na ⁺ [1.8] H ⁺ [1.0]	61	CH ₃ COO ⁻ [1.8]	39										<0.10	<0.10
4	CH ₃ COOH/CH ₃ COONa	4	6.3	Na ⁺ [1.5] H ⁺ [0.1]	52	CH ₃ COO ⁻ [1.5]	48										<0.10	<0.10
5	CH ₃ COOH/CH ₃ COONa	5	7.5	Na ⁺ [642.0] H ⁺ [0.01]	50	CH ₃ COO ⁻ [642.0]	50										<0.10	<0.10
6	CH ₃ COOH/CH ₃ COONa	6	8.1	Na ⁺ [948.0]	50	CH ₃ COO ⁻ [948.0]	50										<0.10	<0.10
7	H ₂ O [reference]	~7															1.44	1.28
8	NaH ₂ PO ₄ /Na ₂ HPO ₄	7	12.9	Na ⁺ [139.0] H ₂ PO ₄ ⁻ [61.0] Na ⁺ [27.8]	84	HPO ₄ ²⁻ [39.0]	16										1.58	0.95
9	NaH ₂ PO ₄ /Na ₂ HPO ₄	7	2.6	Na ⁺ [110.0] HCO ₃ ⁻ [90.0] Na ⁺ [150.0]	84	HPO ₄ ²⁻ [7.8]	16										1.39	1.35
10	NaH ₂ PO ₄ /Na ₂ HPO ₄	8	12.1	H ₂ PO ₄ ⁻ [12.2] Na ⁺ [105.3] H ₂ PO ₄ ⁻ [94.7]	97	HPO ₄ ²⁻ [5.3]	3										1.57	0.80
11	NaHCO ₃ /Na ₂ CO ₃	9	8.6	Na ⁺ [110.0] HCO ₃ ⁻ [90.0] Na ⁺ [150.0]	95	CO ₃ ²⁻ [10.0]	5										1.45	1.37
12	NaHCO ₃ /Na ₂ CO ₃	10	9.5	HCO ₃ ⁻ [50.0] Na ⁺ [190.0] HCO ₃ ⁻ [10.0]	80	CO ₃ ²⁻ [50.0]	20										1.74	1.61
13	NaHCO ₃ /Na ₂ CO ₃	11	10.4	Na ⁺ [100.0]	70	CO ₃ ²⁻ [90.0]	30										1.36	1.30
14	Na ₂ HPO ₄ /Na ₃ PO ₄	12	9.1	Na ⁺ [100.0]	50	HPO ₄ ²⁻ [50.0] PO ₄ ³⁻ [50.0]	50										1.36	1.80

^aThe stability index was determined as the ratio between the number of capsules before and after exposure to specified conditions. ^bPlease refer to Table S3 in the Supporting Information for details.

Table 5. Combined Microscope Imaging and UV–vis Analysis Data for Selected Conditions Listed in Table 4

TMCs	1	2	3	4
			<i>AmT</i> -MCs	
	H ₂ O	NaCl: pH 7 and ppt 9	NaHCO ₃ /Na ₂ CO ₃ : pH 10 and ppt 9.5	Na ₂ HPO ₄ /Na ₃ PO ₄ : pH 12 and ppt 9.1
AUL ^a Ø (µm)	1.28	1.26	1.50	2.03
yield	6.64 ^b	47%	45%	35%
vol. filtrate (mL)	1.20	1.10	1.10	1.05
concentration (mg/mL)	0.006	0.063	0.075	0.050
mass (mg)	0.007	0.069	0.083	0.053
			<i>AmST</i> -MCs	
	H ₂ O	NaH ₂ PO ₄ /Na ₂ HPO ₄ : pH 7 and ppt 12.9	NaH ₂ PO ₄ /Na ₂ HPO ₄ : pH 8 and ppt 12.1	NaHCO ₃ /Na ₂ CO ₃ : pH 10 and ppt 9.5
AUL ^a Ø (µm)	1.44	1.62	1.57	1.70
yield	6.97 ^b	51%	45%	51%
vol. filtrate (mL)	1.20	1.20	1.15	1.05
concentration (mg/mL)	0.006	0.030	0.019	0.020
mass (mg)	0.007	0.036	0.022	0.021

^aAverage upper limit. ^bYield in 10¹² MCs/mL.

that is caused by the high concentrations of hydronium ions at low pH. Higher concentrations of alkali metal ions at higher pH values do not present a destabilizing effect for *AmST*-MCs. These show an ascending stability profile of up to 95% of stable *AmST*-MCs at pH 12. *AmT*-MCs, on the contrary, display a stability profile with an ascending phase from pH 8 to 9 and a descending phase from pH 9 to 12. This interesting difference can be explained by the presence of the sulfonate groups in *AmST*. This confers the system with an additional buffering activity. The sulfonate groups can also interact with the cations and thus minimize/temper their destabilizing effect (vide infra).

In the pH-dependent stability screening, the remaining *AmT*-MCs displayed drastically altered morphological characteristics with respect to the reference sample (Table 3, entries 10 and 14), while *AmST*-MCs did not change equally drastically in morphology.

Given that under different pH conditions, the relative net charge is expected to be distributed throughout the shell, in a first approach, the mechanism of the *AmT*-MC disassembly can be imagined once again (vide supra) as a swelling/bursting process. As indicated by the development of the capsule size in the treatments of TMCs with physiological mixtures and with surfactants, the measured sizes of capsules also suggest, in the case of pH screening, a disintegration upon gradual weakening of the intermolecular electronic interactions, causing different layers of the shell to detach from each other in a centrifugal progressive movement. Additional dedicated experimental work detailed in the Supporting Information supported this hypothesis (Table 5 and Figure 4). These additional experiments also confirmed the invariant aspect ratio of *AmST*-MCs under identical experimental treatments.

Assessment of Salinity-Dependent Stability of TMCs.

The fact that the nature of any salt contents in a TMC solution is at least equally important for TMC stability than the pH, rendering as such the pH discussion only valid to a certain point, was evidenced by two key experiments: at neutral pH, *AmT*-MC robustness has been assessed in the same buffer system, i.e., sodium monophosphate buffer, at two different molarities, i.e., 0.02 and 0.10 M, corresponding to the salinities of 2.6 and 12.9 ppt, respectively. As reported in Table 3, entries 8 and 9, higher salinities lead to the disintegration of 80% of *AmT*-MCs. Therefore, the strong disassembly of *AmT*-MCs observed at pH 7 in the buffer system at 0.1 M must have been

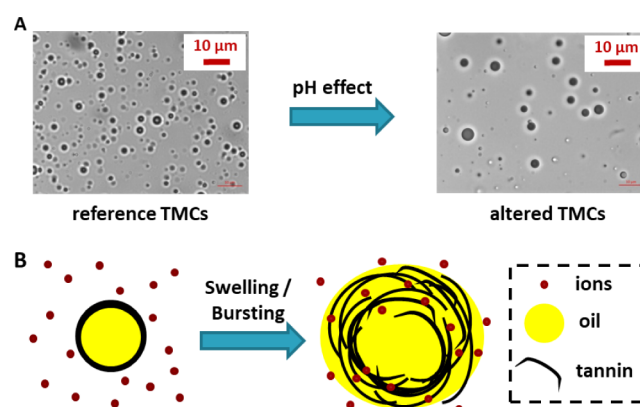


Figure 4. (A) Effect of high pH on *AmT*-MCs and (B) illustration of the swelling/bursting mechanism.

caused by higher salinities, which we eventually additionally potentiated as a function of the chemical nature of the salt.

The generation of the TMC shell structure represents a case in which the intrinsic stacking propensities of tannin and its hydrophobic interactions play a key role.⁸ Consequently, the salt- and salt concentration-dependent stabilities represent TMC reactions toward kosmotropic and chaotropic agents, as traditionally classifiable according to the Hofmeister theories and listed in the Hofmeister series.^{33–36} Chaotropic species should destabilize, whereas kosmotropic agents were expected to have stabilizing effects; mechanistically, ion–dipole interactions between the salts and hydrogen-bonding species are seen as more favorable than normal hydrogen bonds.³⁷ Salt concentrations at which effects are noticeable are usually above 10–100 mM.^{36,38} The chaotropic/kosmotropic effects of physiologically important anions and cations, i.e., PO₄³⁻ > CO₃²⁻ > SO₄²⁻ > CH₃COO⁻ > HPO₄²⁻ > Cl⁻ > H₂PO₄⁻ > HCO₃⁻ and Mg²⁺ > Ca²⁺ > H⁺ > Na⁺ > K⁺, respectively (listed according to the increasing chaotropic nature), were especially interesting in the context of this study.

As reported in Table 6, entries 1, 2, and 19, similar statistical quantitative characteristics of *AmST*-MCs and *AmT*-MCs were observed in deionized H₂O, in the aqueous solutions of Na₂HPO₄ and MOPS at pH 7 and salinities of 10 and 21 ppt, respectively. In contrast, 35% and 75% of *AmST*-MCs were lost in aqueous PBS and KCl solutions at pH 7 and a salinity of 10 ppt (Table 6, entries 10 and 11). Similar numbers were

Table 6. Assessment of the Salinity-Dependent Stability of AmST-MCs and AmT-MCs^a

entry	medium	salinity (ppt)	pH	molarity (mM)	chaotropic (mM)	chaotropic (%)	kosmotropic (mM)	kosmotropic (%)	AUL ϕ (μm)		PDI		# MCs (10^{12} MCs/m ³ L)		stability index		
									AmST	AmT	AmST	AmT	AmST	AmT	AmST	AmT	AmST
1	H ₂ O [reference]		~7							1.44	1.28	0.5	0.5	6.97	6.64	1.00	1.00
2	NaH ₂ PO ₄ /Na ₂ HPO ₄	2.6	7	20.0	Na ⁺ [27.8] H ₂ PO ₄ ⁻ [12.2]	84	HPO ₄ ²⁻ [7.8]	16		1.39	1.35	0.5	0.5	6.90	6.71	0.99	1.01
3	NaCl	5	~7	85.6	Na ⁺ [85.6] Cl ⁻ [85.6]	100				1.29	1.28	0.5	0.6	5.97	6.24	0.86	0.94
4	KCl/HCl	4.8	1	100.0	H ⁺ [100.0] K ⁺ [29.0] Cl ⁻ [100.0]	100										<0.10	<0.10
5	CH ₃ COOH/CH ₃ COONa	8.1	6	100.0	Na ⁺ [94.8]	50	CH ₃ COO ⁻ [94.8]	50								<0.10	<0.10
6	NaHCO ₃ /Na ₂ CO ₃	8.6	9	100.0	Na ⁺ [100.0] HCO ₃ ⁻ [90.0]	95	CO ₃ ²⁻ [10.0]	5		1.45	1.37	0.4	0.6	2.86	5.78	0.41	0.87
7	NaCl	9	~7	154.1	Na ⁺ [154.1] Cl ⁻ [154.1]	100				1.37	1.46	0.4	0.5	3.83	4.98	0.55	0.75
8	Na ₂ HPO ₄ /Na ₃ PO ₄	9.1	12	100.0	Na ⁺ [100.0]	50	HPO ₄ ²⁻ [50.0] PO ₄ ³⁻ [50.0]	50		1.36	1.50	0.4	0.6	6.62	1.99	0.95	0.30
9	NaHCO ₃ /Na ₂ CO ₃	9.5	10	100.0	Na ⁺ [150.0] HCO ₃ ⁻ [50.0]	80	CO ₃ ²⁻ [50.0]	20		1.74	1.61	0.3	0.5	2.79	3.92	0.40	0.59
10	PBS	9.9	~7	100.0	Na ⁺ [157.3] K ⁺ [4.4] Cl ⁻ [139.7]	97	HPO ₄ ²⁻ [10.1]	3		1.41	1.35	0.4	0.3	4.53	4.85	0.65	0.73
11	KCl	10	~7	134.1	H ₂ PO ₄ ⁻ [1.8] K ⁺ [134.1] Cl ⁻ [134.1]	100				1.09	1.25	0.6	0.5	1.60	1.66	0.23	0.25
12	CaCl ₂	10	~7	90.1	Cl ⁻ [180.2]	67	Ca ²⁺ [90.1]	33								<0.10	<0.10
13	MgSO ₄	10	~7	80.1	Cl ⁻ [180.2]	100	Mg ²⁺ [80.1] SO ₄ ²⁻ [80.1]	100								<0.10	<0.10
14	Na ₂ HPO ₄	10	7	70.4	Na ⁺ [140.9]	67	HPO ₄ ²⁻ [70.4]	33		1.42	1.32	0.5	0.5	6.26	5.71	0.89	0.86
15	NaHCO ₃ /Na ₂ CO ₃	10.4	11	100.0	Na ⁺ [190.0] HCO ₃ ⁻ [10.0]	70	CO ₃ ²⁻ [90.0]	30		1.36	1.30	0.3	0.5	3.21	3.45	0.46	0.52
16	NaH ₂ PO ₄ /Na ₂ HPO ₄	12.1	8	100.0	Na ⁺ [105.3] H ₂ PO ₄ ⁻ [94.70]	97	HPO ₄ ²⁻ [5.3]	3		1.57	0.80	0.5	0.4	2.58	4.12	0.37	0.62
17	NaH ₂ PO ₄ /Na ₂ HPO ₄	12.9	7	100.0	Na ⁺ [139.0] H ₂ PO ₄ ⁻ [61.0]	84	HPO ₄ ²⁻ [39.00]	16		1.58	0.95	0.4	0.4	1.18	1.26	0.17	0.19
18	NaCl	15	~7	256.9	Na ⁺ [256.9] Cl ⁻ [256.9]	100				1.46	1.32	0.4	0.6	3.27	3.65	0.46	0.55
19	MOPS	21	~7	100.0						1.35	1.31	0.4	0.6	6.93	6.56	0.99	0.90
20	SDS	29	~7	100.0						1.38	1.38	0.4	0.4	3.65	5.28	0.55	0.76

^aThe stability index was determined as a ratio between the number of capsules before and after exposure to specified conditions.

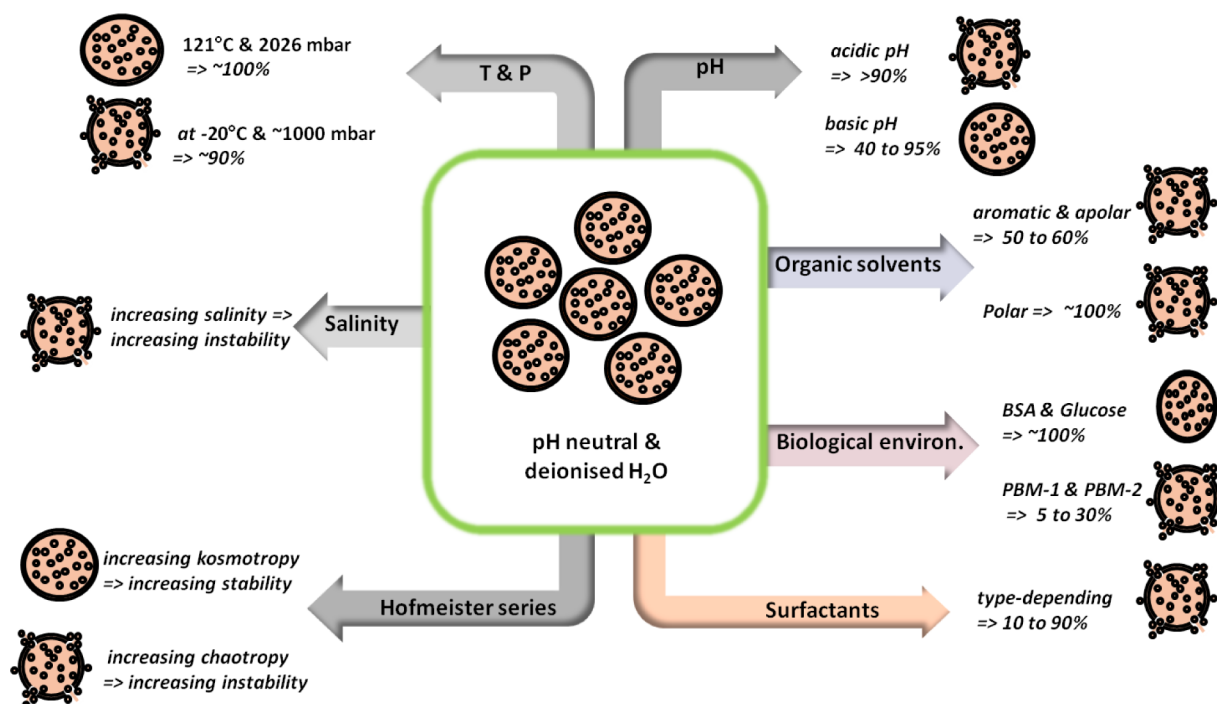


Figure 5. Overview summarizing TMC stabilities under various conditions.

found for *AmT*-MCs under identical conditions and time-frames. These results suggest the applicability of the Hofmeister series for predictions regarding the TMC stability: phosphate ions as strong kosmotropic agents should have a stabilizing effect. Chloride anions, on the contrary, known as an borderline kosmotropic/chaotropic agent, are expected to be more detrimental than beneficial. In the case of PBS, the phosphate anion as strong kosmotropic agent compensates for the chaotropic effects of the chloride ions. This compensatory effect is confirmed by the increasing stability profile of *AmST*-MCs alongside with an increasing proportion of phosphates and/or carbonates in alkaline environments (Table 6, entries 10–14).

At neutral pH, 6%, 25%, and 45% of *AmT*-MCs were disassembled, respectively, after 48 h in aqueous NaCl solutions at 5, 9, and 15 ppt, respectively (Table 6, entries 3, 7, and 18).

The phenomenon of decreasing stability with increasing salinity is also generally seen in buffer systems containing both chaotropic and kosmotropic agents. One example is the phosphate buffer system containing 84% of chaotropic agents, sodium and dihydrogen phosphate ions, and only 16% of a moderately kosmotropic agent, i.e., hydrogen phosphate. As it can be observed in Table 6, entries 2 and 17, in the same type of buffer system by simply augmenting the buffering capacity from 0.02 to 0.1 M, corresponding to an increase in the salinity from 2.6 to 12.9 ppt, *AmT*-MCs display similar statistical key figures in both deionized H₂O and in the solution with a salinity of 2.6 ppt; at a 6-fold increased salinity of 12.9 ppt, more than 80% of *AmST*-MCs and *AmT*-MCs were disassembled.

At different pH values, i.e., pH 1 and pH 7 (Table 6, entries 4 and 11), >90% and ~75% of *AmT*-MCs and *AmST*-MCs were disassembled in aqueous KCl solutions at a salinity of 4.8 and 10 ppt, respectively. These results indicate that in an acidic environment, the chaotropic potential is more effective even at

a relatively low salinity. The reinforcement of the chaotropic potential by the acidic environment is also seen in buffer systems with the same proportion of both chaotropic and kosmotropic agents.

Alkaline earth metals in the dicationic form lead to the rapid disintegration of more than 90% of TMCs independently of the nature of the tannin used for shell construction (neutral pH in 0.09 M solutions of CaCl₂ and MgSO₄ at 10 ppt salinity, Table 6, entries 12 and 13).

In the aqueous solutions of MOPS (21 ppt), *AmST*-MCs show excellent stability in higher salinity environments, and even *AmT*-MCs are rather stable; as indicated in the screening of surfactant-induced TMC disintegration, SDS (29 ppt) causes a more rapid decline in TMC numbers (Table 6, entries 19 and 20).

CONCLUSIONS

MCs formed from *AmST*-MCs were synthesized for the first time using a sonochemical approach applied to water/oil emulsions. The process for both the sulfited and nonsulfited *Acacia mearnsii* tannin MC generation has been reoptimized with respect to effectiveness and scalability. The novel *AmST*-MCs show comparable morphological characteristics when compared to *AmT*-MCs generated accordingly from the nonsulfited *Acacia mearnsii* tannin extract.

Both types of tannin-based MCs exhibit excellent stability over time, under high temperature and pressure (autoclaving conditions) when kept in pure water solutions. They also display excellent to very good stability in the presence of some excipients and organic macromolecules. Stimuli-triggered disassembly can be induced by variation of pH, with the possibility for fast releases at acidic pH and rather slow releases at alkaline pH ranges especially in case of *AmST*-MCs. The salinity of the medium surrounding the capsules was found to be a powerful tool to trigger capsule disassembly and thus active release. Also here, *AmST*-MCs were found to be the

more stable species overall, especially at neutral pH. Surfactants also affect the stability of TMCs significantly, the effect of which is eventually amplifiable by pH and salinity variation.

The intrinsic stacking propensities of tannins and their hydrophobic interactions, in general, guarantee the successful generation of the TMC shells.^{8,9} Chao- or kosmotropic nature of salts thus has an effect on polyphenol-based nanostructures. In this respect, the study showed that, except in the case of the kosmotropic dicationic agents, the analytical data are by and large in line with the expected cumulative disassociating effect of chaotropic agents and the associating effect of the kosmotropic agents.

The study also reveals, however, the complexity of the effects and interactions caused by salinity, pH, and Hofmeister characteristics. Figure 5 summarizes the findings described in this study and is considered as a rough guide for choosing the presumably most appropriate tannin for the intended application.

MATERIALS AND METHODS

General Information. Chemicals, salts, and solvents were purchased from Sigma-Aldrich or Carlo Erba in appropriate grades and were used without further purification if not stated otherwise. Sulfited *Acacia mearnsii* tannin (*AmST*) and *Acacia mearnsii* bark extract (*AmT*) were obtained from Silvachimica s.r.l.

Preparation of the Aqueous *AmST* and *AmT* solutions. In an optimized procedure, 0.5% w/w of aqueous *AmST* and *AmT* solutions were prepared by suspending 100.0 mg of *AmST* or *AmT* in 20.0 mL of distilled H₂O and by adding some drops of aqueous 1 M NaOH to bring the systems to pH ~12.

Preparation of Starting Emulsion and Generation of TMCs. Five hundred microliters of the aqueous *AmST* or *AmT* solutions were mixed with 500 μ L of olive oil. This biphasic system was magnetically stirred for 5 min. Using a Branson Digital Sonifier Model 450L (Ultrasonic Corporation) equipped with a 20 kHz Branson probe ending in a sonication tip, the mixture was then ultrasonicated at room temperature (RT) with a power of 160 W (40% amplitude) for 10 min.

Isolation of TMCs. The isolation of the TMCs from the remaining liquid was realized by centrifugation of the emulsion obtained after sonication at 5000 rpm for 15 min. The lower aqueous phase was removed, and the foamy supernatant in TMCs was washed, as follows, to remove the residual tannin and oil. "Washing" consisted of resuspending the TMCs in 1000 μ L of distilled H₂O before repeating the centrifugation and phase separation step, as previously described. This "washing" was performed at least twice to obtain the "concentrated" TMCs. The pH of these "concentrated," i.e., densely packed, TMCs was ~7.

Preparation of the Aqueous Solutions Containing Chemical Triggers. Buffer solutions, salt solutions, surfactant solutions, and aqueous solutions containing carbohydrates and proteins were prepared exactly as described in great detail before.²⁴ Table S3 lists the used buffer systems in detail again.

Screening of TMC Disassembly in Various Aqueous Media. Ten microliters of the generated "concentrated" TMCs were dispersed in an Eppendorf tube containing 990 μ L of the medium in which the stability of the TMCs was to be determined. TMCs were dispersed homogeneously by gently shaking the system for 2 min. The system was then observed

for eventual macroscopical changes in its consistency, before it was kept under various conditions for the indicated times with the occasional redispersing of the eventually settled TMCs. The system was gently shaken again, and an aliquot was taken and analyzed via optical microscopy as discussed below.

Temperature- and Pressure-Triggered Release Screening. Ten microliters of the "concentrated" TMCs was dispersed in 990 μ L of distilled H₂O in an Eppendorf tube suitable for high temperatures. An aliquot was analyzed via optical microscopy before and after the freezing and the heating processes. The samples were frozen at -20 °C at standard pressure (~1000 mbar) for 1 week; heat tests were performed in an autoclave at 121 °C at 2026 mbar for 30 min.

UV-Vis Analysis. Sample Preparation. Ten microliters of the generated "concentrated" TMCs were dispersed in an Eppendorf tube containing 990 μ L of the medium in which the stability of the TMCs was to be determined. TMCs were dispersed homogeneously by gently shaking the system for 2 min. After the microscope analysis, the system was filtered off and the filtrate was used for UV-vis analysis.

Optical Microscopy Analysis and Statistical Analysis. A procedure similar to the ones established before was used.^{8,9}

Sample Preparation. Ten microliters of the generated "concentrated" TMCs was added in 990 μ L of distilled H₂O to form a suspension of TMCs. Five 5 microliters of this suspension was transferred on a microscope carrier glass slide and covered with a coverslip prior to microscopy analysis. In case the capsules significantly overlap, the sample should be further diluted, prior to analysis.

Analysis. A Zeiss Axio Scope A1 microscope was used for image analysis. All images were obtained with 100 \times objective lens magnification. For optimizing the exploitation of the 100 \times lens, a drop of mineral oil was placed on the coverslip prior to the analysis to function as an optical bridge.

Processing. The pictures from the microscope were processed using the image analysis software ImageJ in combination with Microsoft Office Excel based analyses, as described in detail before. Three microscopic images were chosen for ImageJ-based analysis; settings of the program parameters for picture analysis were chosen such as to ensure that all capsules visible in the image were recognized by the software, accounting as such for differences in microscope picture brightness. Error analysis was performed according to this protocol using 10 different samples. A comparison between a manual counting and an ImageJ software-based counting has been accomplished by screening different settings in the software. Based on these various evaluations regarding the quality of the computer-based analysis, average errors were estimated for the average upper limits of diameters and the number of MCs per milliliter: 0.08 μ m and 0.17 $\times 10^{12}$ MCs/mL, respectively.

ASSOCIATED CONTENT

Supporting Information

The Supporting Information is available free of charge at <https://pubs.acs.org/doi/10.1021/acsomega.1c01065>.

Three tables containing additional data (Table S1–S3) and six additional figures (Figures S1–S6) (PDF)

AUTHOR INFORMATION

Corresponding Authors

Heiko Lange – Department of Earth and Environmental Sciences, University of Milano-Bicocca, Milan 20126, Italy; CSGI – Center for Colloid and Surface Science, Florence 50019, Italy; orcid.org/0000-0003-3845-7017; Email: heiko.lange@unimib.it

Claudia Crestini – Department of Molecular Science and Nanosystems, University of Venice “Ca’ Foscari”, Venice Mestre 30170, Italy; CSGI – Center for Colloid and Surface Science, Florence 50019, Italy; orcid.org/0000-0001-9903-2675; Email: claudia.crestini@unive.it

Author

Luc Zongo – Department of Chemical Science and Technologies, University of Rome “Tor Vergata”, Rome 00133, Italy

Complete contact information is available at:

<https://pubs.acs.org/10.1021/acsomega.1c01065>

Author Contributions

#Affiliated with Department of Chemical Science and Technologies, University of Rome “Tor Vergata” via NAST – Nanoscience & Nanotechnology & Innovative Instrumentation Center.

Author Contributions

L.Z. was involved in investigation and writing—original draft preparation; H.L. was involved in conceptualization, methodology, supervision, data curation, writing—original draft preparation, and writing—reviewing and editing; and C.C. was involved in funding, conceptualization, methodology, supervision, data curation, and writing—reviewing and editing. All authors have given approval to the final version of the manuscript.

Notes

The authors declare no competing financial interest.

ACKNOWLEDGMENTS

Silvachimica s.r.l. in Italy is acknowledged for generously providing the samples of commercialized Acacia tannins.

ABBREVIATIONS

AE	alcohol ethoxylate
AmT	<i>Acacia mearnsii</i> bark extract tannins
AmT-MCs	<i>Acacia mearnsii</i> bark extract tannin microcapsules
AmST	<i>Acacia mearnsii</i> sulfited tannins
AmST-MCs	<i>Acacia mearnsii</i> sulfited tannin microcapsules
AO	amine oxide
BSA	bovine serum albumin
MOPS	(3-(<i>N</i> -morpholino)propanesulfonic acid
MCs	microcapsules
PBS	phosphate-buffered saline
RT	room temperature
SDS	sodium dodecyl sulfate
STMCs	sulfited tannin microcapsules
TMCs	tannin microcapsules
UV-vis	ultraviolet-visible

REFERENCES

(1) Nazzaro, F.; Orlando, P.; Fratianni, F.; Coppola, R. Microencapsulation in Food Science and Biotechnology. *Curr. Opin. Biotechnol.* **2012**, *23*, 182–186.

(2) Li, M.; Rouaud, O.; Poncelet, D. Microencapsulation by Solvent Evaporation: State of the Art for Process Engineering Approaches. *Int. J. Pharm.* **2008**, *363*, 26–39.

(3) Park, J.; Ye, M.; Park, K. Biodegradable Polymers for Microencapsulation of Drugs. *Molecules* **2005**, *10*, 146–161.

(4) Singh, M. N.; Hemant, K. S. Y.; Ram, M.; Shivakumar, H. G. Microencapsulation: A Promising Technique for Controlled Drug Delivery. *Res. Pharm. Sci.* **2010**, *5*, 65–77.

(5) Tomaro-Duchesneau, C.; Saha, S.; Malhotra, M.; Kahouli, I.; Prakash, S. Microencapsulation for the Therapeutic Delivery of Drugs, Live Mammalian and Bacterial Cells, and Other Biopharmaceuticals: Current Status and Future Directions. *J. Pharm. (Cairo)* **2013**, *2013*, No. 103527.

(6) Suganya, V.; Anuradha, V. Microencapsulation and Nanoencapsulation: A Review. *IJPCR* **2017**, *9*, 233–239.

(7) *Microencapsulation: Methods and Industrial Applications*, 2nd ed.; Benita, S., Ed.; CRC Press, 2005.

(8) Bartzoka, E. D.; Lange, H.; Mosesso, P.; Crestini, C. Synthesis of Nano- and Microstructures from Proanthocyanidins, Tannic Acid and Epigallocatechin-3-O-Gallate for Active Delivery. *Green Chem.* **2017**, *19*, 5074–5091.

(9) Bartzoka, E. D.; Lange, H.; Poce, G.; Crestini, C. Stimuli-Responsive Tannin-FeIII Hybrid Microcapsules Demonstrated by the Active Release of an Anti-Tuberculosis Agent. *ChemSusChem* **2018**, *11*, 3975–3991.

(10) Kozlovskaya, V.; Kharlampieva, E.; Drachuk, I.; Cheng, D.; Tsukruk, V. Responsive Microcapsule Reactors Based on Hydrogen-Bonded Tannic Acid Layer-by-Layer Assemblies. *Soft Matter* **2010**, *6*, 3596–3608.

(11) Huang, H.; Li, P.; Liu, C.; Ma, H.; Huang, H.; Lin, Y.; Wang, C.; Yang, Y. PH-Responsive Nanodrug Encapsulated by Tannic Acid Complex for Controlled Drug Delivery. *RSC Adv.* **2017**, *7*, 2829–2835.

(12) Liu, F.; Kozlovskaya, V.; Zavgorodnya, O.; Martinez-Lopez, C.; Catledge, S.; Kharlampieva, E. Encapsulation of Anticancer Drug by Hydrogen-Bonded Multilayers of Tannic Acid. *Soft Matter* **2014**, *10*, 9237–9247.

(13) Rahim, M. A.; Ejima, H.; Cho, K. L.; Kempe, K.; Müllner, M.; Best, J. P.; Caruso, F. Coordination-Driven Multistep Assembly of Metal-Polyphenol Films and Capsules. *Chem. Mater.* **2014**, *26*, 1645–1653.

(14) Lomova, M. V.; Brichkina, A. I.; Kiryukhin, M. V.; Vasina, E. N.; Pavlov, A. M.; Gorin, D. A.; Sukhorukov, G. B.; Antipina, M. N. Multilayer Capsules of Bovine Serum Albumin and Tannic Acid for Controlled Release by Enzymatic Degradation. *ACS Appl. Mater. Interfaces* **2015**, *7*, 11732–11740.

(15) Ejima, H.; Richardson, J. J.; Liang, K.; Best, J. P.; van Koeven, M. P.; Such, G. K.; Cui, J.; Caruso, F. One-Step Assembly of Coordination Complexes for Versatile Film and Particle Engineering. *Science* **2013**, *341*, 154–157.

(16) Khanbabaee, K.; Van Ree, T. Tannins: Classification and Definition. *Nat. Prod. Rep.* **2001**, *18*, 641–649.

(17) Pizzi, A. Chapter 8 - Tannins: Major Sources, Properties and Applications. In *Monomers, Polymers and Composites from Renewable Resources*; Belgacem, M. N., Gandini, A., Eds.; Elsevier: Amsterdam, 2008; pp 179–199.

(18) Serrano, J.; Puupponen-Pimiä, R.; Dauer, A.; Aura, A.-M.; Saura-Calixto, F. Tannins: Current Knowledge of Food Sources, Intake, Bioavailability and Biological Effects. *Mol. Nutr. Food Res.* **2009**, *53*, S310–S329.

(19) Wang, S.; Melnyk, J. P.; Tsao, R.; Marcone, M. F. How Natural Dietary Antioxidants in Fruits, Vegetables and Legumes Promote Vascular Health. *Food Res. Int.* **2011**, *44*, 14–22.

(20) Pizzi, A. Tannins: Prospectives and Actual Industrial Applications. *Biomolecules* **2019**, *9*, 344.

(21) García, D. E.; Glasser, W. G.; Pizzi, A.; Paczkowski, S. P.; Laborie, M.-P. Modification of Condensed Tannins: From Polyphenol Chemistry to Materials Engineering. *New J. Chem.* **2016**, *40*, 36–49.

(22) *Cavitation: A Novel Energy-Efficient Technique for the Generation of Nanomaterials*, 1st ed.; Manickam, S., Ashokkumar, M., Eds.; Jenny Stanford Publishing: New York, 2014.

(23) Leong, T.; Ashokkumar, M.; Kentish, S. The Fundamentals of Power Ultrasound—A Review. *Acoust. Aust.* **2011**, *39*, 54–63.

(24) Zongo, L.; Lange, H.; Crestini, C. A Study of the Effect of Kosmotropic and Chaotropic Ions on the Release Characteristics of Lignin Microcapsules under Stimuli-Responsive Conditions. *ACS Omega* **2019**, *4*, 6979–6993.

(25) Vázquez, G.; Freire, M. S.; González-Álvarez, J.; Antorrena, G. Valorisation of Lignocellulosic Waste Materials: Tannins as a Source of New Products. *Proceedings of European Congress of Chemical Engineering (ECCE-6)*, Copenhagen, September 16–20, 2007.

(26) González-García, S.; Lacoste, C.; Aicher, T.; Feijoo, G.; Lijó, L.; Moreira, M. T. Environmental Sustainability of Bark Valorisation into Biofoam and Syngas. *J. Cleaner Prod.* **2016**, *125*, 33–43.

(27) Lebo, S. E., Jr.; Detroit, W. J. Method for Microencapsulation of Agriculturally Active Substances. *US5552149A*, September 3, 1996

(28) Noreljaleel, A. E. M.; Kemp, G.; Wilhelm, A.; Van Der Westhuizen, J. H.; Bonnet, S. L. Analysis of Commercial Proanthocyanidins. Part 5: A High Resolution Mass Spectrometry Investigation of the Chemical Composition of Sulfited Wattle (*Acacia mearnsii* De Wild.) Bark Extract. *Phytochemistry* **2019**, *162*, 109–120.

(29) Crestini, C.; Lange, H.; Bianchetti, G. Detailed Chemical Composition of Condensed Tannins via Quantitative ³¹P NMR and HSQC Analyses: *Acacia catechu*, *Schinopsis balansae*, and *Acacia mearnsii*. *J. Nat. Prod.* **2016**, *79*, 2287–2295.

(30) Bartzoka, E. D.; Lange, H.; Thiel, K.; Crestini, C. Coordination Complexes and One-Step Assembly of Lignin for Versatile Nanocapsule Engineering. *ACS Sustainable Chem. Eng.* **2016**, *4*, 5194–5203.

(31) Sharp, K. A.; Honig, B. Electrostatic Interactions in Macromolecules: Theory and Applications. *Ann. Rev. Biophys. Biophys. Chem.* **1990**, *19*, 301–332.

(32) McPhail, A. T.; Sim, G. A. Hydroxyl–Benzene Hydrogen Bonding: An X-Ray Study. *Chem. Commun. (London)* **1965**, 124–126.

(33) Hofmeister, F. Zur Lehre von Der Wirkung Der Salze. *Naunyn-Schmiedeberg's Arch. Pharmacol.* **1888**, *25*, 1–30.

(34) Kunz, W.; Henle, J.; Ninham, B. W. 'Zur Lehre von Der Wirkung Der Salze' (about the Science of the Effect of Salts): Franz Hofmeister's Historical Papers. *Curr. Opin. Colloid Interface Sci.* **2004**, *9*, 19–37.

(35) Peruzzi, N.; Ninham, B. W.; Lo Nostro, P.; Baglioni, P. Hofmeister Phenomena in Nonaqueous Media: The Solubility of Electrolytes in Ethylene Carbonate. *J. Phys. Chem. B* **2012**, *116*, 14398–14405.

(36) Lo Nostro, P.; Ninham, B. W. Hofmeister Phenomena: An Update on Ion Specificity in Biology. *Chem. Rev.* **2012**, *112*, 2286–2322.

(37) Collins, K. D. Charge Density-Dependent Strength of Hydration and Biological Structure. *Biophys. J.* **1997**, *72*, 65–76.

(38) *Molecular Forces and Self Assembly: In Colloid, Nano Sciences and Biology*; Ninham, B. W., Nostro, P. L., Eds.; Cambridge University Press, 2010.